Single-Chain Nanoparticles with Well-Defined Structure via Intramolecular Crosslinking of Linear Polymers with Pendant Benzoxazine Groups

Peng Wang, Hongting Pu, Ming Jin

Institute of Functional Polymers, School of Materials Science and Engineering, Tongji University, Shanghai 201804, China
Correspondence to: H. Pu (E-mail: puhongting@tongji.edu.cn)

Received 27 August 2011; accepted 9 September 2011; published online 26 September 2011
DOI: 10.1002/pola.25003

ABSTRACT: Controlled intramolecular collapse of linear polymer chains with crosslinkable groups is an efficient way to prepare single-chain nanoparticles in the size range of 5–20 nm. However, the nature of the crosslinking group is critical. In present study, poly(styrene-*co*-chloromethyl styrene) [P(St-*co*-CMS)] was synthesized via reversible addition-fragmentation chain transfer (RAFT) polymerization and then was converted into polystyrene azide (PS—N_3). Polystyrene containing benzoxazine side groups [P(St-*co*-BS)], which can be used as the precusor for the later intramolecular collapse, was obtained from PS—N_3 and 3-(4-(prop-2-ynyloxy)phenyl)-3,4-dihydro-2H-benzo [e][1,3]oxazine (P-APPE) via the method of click chemistry. The sub-20 nm polymeric nanoparticles with well-defined structure via thermally intramolecular crosslinking of P(St-*co*-BS) were prepared. The structure change from the linear polymers to the single-chain nanoparticles was confirmed by nuclear magnetic resonance (NMR), Fourier transform infrared (FTIR), and gel permeation chromatography (GPC). The morphology and the dimension of the nanoparticles were characterized by using transmission electron microscope (TEM), atomic force microscopy (AFM), as well as dynamic light scattering (DLS). The results reveal that the size of the nanoparticles can be regulated by changing the molecular weight of the precursors and the amount of pendant benzoxazine groups by the use of controlled polymerization techniques. © 2011 Wiley Periodicals, Inc. J Polym Sci Part A: Polym Chem 49: 5133–5141, 2011

KEYWORDS: benzoxazine; crosslinking; nanoparticles; reversible addition fragmentation chain transfer (RAFT); single-chain

INTRODUCTION Polymer nanoparticles have attracted significant attention in recent years due to their peculiar properties and key role in the implementation of nanotechnology. Compared with inorganic nanoparticles, polymeric nanoparticles as a kind of soft materials show better biocompatibility, biodegradability, and self-assembly performance. Thus, functionalized polymer nanoparticles can be considered as building blocks for a variety of nanotechnological applications, ranging from vectors for drug and DNA delivery systems[1,2] to templating agents for nanoporous microelectronic materials.[3] Among the technologies developed to prepare polymer nanoparticles, two types of methods are conventionally used. One is the dispersion of preformed polymers, including microphase inversion,[4] nanopreciptation,[5] self-assembly of block copolymers into micelles followed by chemical crosslinking (20–200 nm),[6] as well as supramolecular strategies to collapse nanoparticles.[2,7] The other is the polymerization of monomers in dispersed medium, such as emulsion polymerization (50–200 nm), microemulsion technique (20–50 nm),[8] as well as the synthesis of discrete spherical macromolecules like dendrimers (1–10 nm), which has the disadvantages of complicated synthetic procedure and too much byproducts.[9] As a consequence, polymer nanoparticles with size ranging from 20 to 200 nm can be effectively obtained using these methods, but the preparation of smaller nanoparticles is still challenging.

A strategy involving the collapse and intramolecular coupling of polymeric single-chain to give discrete nanoparticle in the size range of 5–20 nm has been proposed.[10] Synthetically, the preparation of these polymeric nanoparticles involves two steps. The first involves the synthesis of crosslinkable linear polymers. They can be the polymers with reactive groups which can be thermally or chemically crosslinked later. Up to date, this technique includes crosslinking of vinyl functionalization,[11] click chemistry,[12] thermal crosslinking of benzylcyclobutane,[13] or sulfonyl azide,[14] crosslinking of alternate o-quinodimethane precursors,[15] crosslinking of copolymers containing pendent isocyanate functionality with diamine,[16] photo-crosslinking of cinnamoyl groups,[17] to give the single-chain nanoparticles. The second involves the preparation of single-chain nanoparticles in ultra-dilute solution (ca.10^{-5}–10^{-6} M) to avoid intermolecular crosslinking reaction. But this precludes the synthesis of these nanoparticles in mass. In addition, even at this ultra-diluted solution

Additional Supporting Information may be found in the online version of this article.

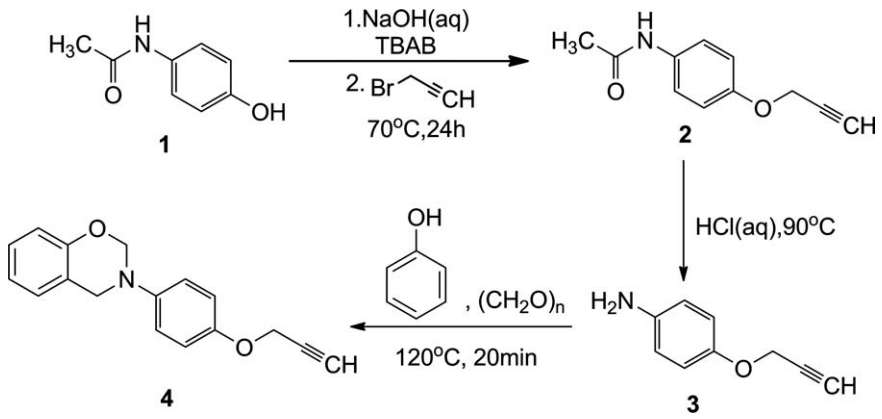

SCHEME 1 Synthesis of 3-(4-(prop-2-ynyloxy)phenyl)-3,4-dihydro-2H-benzo[e][1,3]oxazine.

intermolecular crosslinking is still evident, which results in poorly defined structure and even gelation in some cases. To overcome this difficulty, a continuous dropwise addition strategy for the successful synthesis of discrete nanoparticles was proposed.[13,14] In this way, intermolecular crosslinking can be effectively eliminated even at high concentration (0.1 M), which makes it a practical technique for the large-scale synthesis of well-defined nanoparticles.

To satisfy these demands, the nature of the crosslinking group is critical. It must be selectively activated and react rapidly, leading to the efficient formation of the intramolecular bonds. It is also important that this reaction is irreversible and leads to a bonded structure that is subsequently unreactive under the reaction condition.[13] However, most of the crosslinking reactions are difficulty to be controlled and have subsidiary reactions, which produce the nanoparticles with complicated structure and wide dispersion.[11,14,17] Benzoxazines are heterocyclic compounds which can be polymerized via a thermally induced ring-opening polymerization without using any catalyst and thus no other byproducts are generated during the polymerization. Furthermore, benzoxazine monomers can be easily prepared from inexpensive raw materials like phenols, formaldehyde, and primary amines (aliphatic or aromatic) either via solution or solventless method.[18] Accordingly, various types of benzoxazine monomers can be synthesized using various phenols and amines with different substituting groups attached. These substituting groups can provide additional polymerizable sites and also affect the crosslinking process.[19]

In this study, propargyl ether functionalized benzoxazine monomer was synthesized and added to azide functionalized polymers via the method of click chemistry to give the crosslinkable linear polymers. These linear polymers can undergo intramolecular collapse by ring-opening polymerization of benzoxazine groups to give polymer nanoparticles with small size. Furthermore, the polymer nanoparticles obtained from this procedure are freely soluble in common solvents and do not need any surfactant, during either the synthesis or the subsequent stabilization of the resulting nanoparticle solution.

RESULTS AND DISCUSSION

Synthesis of Propargyl Ether Functionalized Benzoxazine

Propargyl ether functionalized benzoxazine, 3-(4-(prop-2-ynyloxy)phenyl)-3,4-dihydro-2H-benzo[e][1,3]oxazine (P-APPE), was synthesized from phenol, paraformaldehyde with p-aminophenyl propargyl ether (APPE) by solventless method according to Scheme 1. The chemical structure of P-APPE (**4**) was confirmed by both FTIR and ^{1}H NMR. The characteristic absorption of benzoxazine structure appears at 1,217 cm^{-1} due to the asymmetric stretching of C—O—C, and the peaks at 954 and 1,506 cm^{-1} are attributed to the tri-substituted benzene ring. The propargyl group is evidenced by characteristic bands of H—C≡C and —C≡C— appeared at 3,286 and 2,121 cm^{-1}, respectively. ^{1}H NMR spectrum of P-APPE shows a triplet at 2.50 ppm and a doublet at 4.55 ppm, which are assigned to H—C≡ and CH_2 (propargyl). Also, the protons on N—CH_2—O and N—CH-Ar of oxazine rings are detectable at 5.29 and 4.61 ppm.

Synthesis of Linear Polystyrene Containing Pendent Benzoxazine Groups

For the synthesis of parent azide functionalized copolymers, a series of poly(styrene-*co*-chloromethyl styrene) (P(St-*co*-CMS)), **5** were first prepared via reversible addition-fragmentation chain transfer (RAFT) polymerization of chloromethyl styrene (CMS) and styrene (St) in the presence of S-ethoxycarbonyl phenylmethyl dithiobenzoate (ECPDB) and azobisisobutyronitrile (AIBN) according to Scheme 2. The composition of the copolymer was determined using ^{1}H NMR spectroscopy. The mole fractions of CMS and St are calculated from the ratio of the peak area around 4.5 ppm, corresponding to two protons of methylene in the side chain of CMS, to the total area between 6.25 and 7.24 ppm, which is attributed to the total aromatic protons. Then copolymer **5** with different mole fraction of chloromethyl groups (5–20 mol %) is quantitatively converted into polystyrene azide (PS—N_3) (**6**) in the presence of NaN_3/*N*,*N*-dimethylformamide (DMF) at room temperature. From ^{1}H NMR spectrum of **6** shown in Figure 1(A), it can be found that a new signal appears at 4.25 ppm due to CH_2 linked to azide groups when the signal at 4.5 ppm, corresponding to the protons of

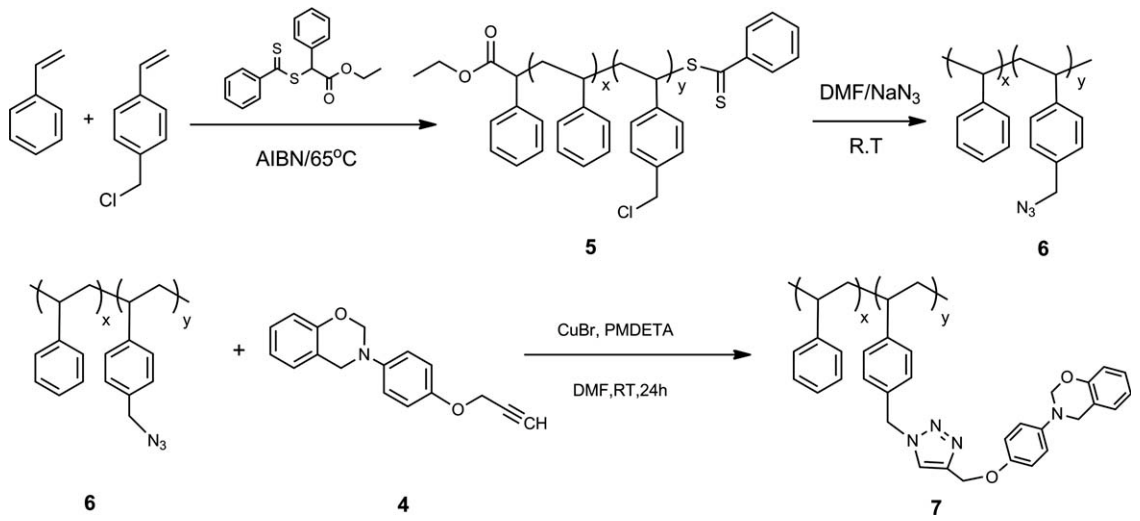

SCHEME 2 Synthesis of linear polymers containing pendent benzoxazine functionalities.

CH_2-Cl in copolymer **5**, disappears completely. The structure of **6** is further supported by the observation from IR spectrum of the azide stretching band at 2,096 cm^{-1} [Fig. 2(A)].

Click chemistry is an effective method to join small modular units together.[20] Thus polystyrene containing benzoxazine side groups [P(St-*co*-BS)] can be obtained from PS—N_3 and P-APPE via the method of click chemistry, as shown in Scheme 2. PS—N_3 (**6**) was dissolved in DMF and reacted with **4** in the presence of CuBr/*N*,*N*,*N*′,*N*″,*N*″-pentamethyldiethylenetriamine (PMDETA) ligand at room temperature under nitrogen. After removing the catalyst, the polymer was precipitated and dried under vacuum. The extent of conversion of the side azide moieties was monitored by ^{1}H NMR and by observing the disappearance of the protons of methylene adjacent to the azide group (N_3—CH_2Ph) at 4.25 ppm as well as the appearance of the new protons of methylene adjacent to the triazole ring at 5.36 ppm (triazole-CH_2Ph) [Fig. 1(B)]. Moreover, the band, corresponding to the —N_3 group at 2,096 cm^{-1}, disappears completely [Fig. 2(B)]. Thus, the click reaction of the side group is efficient, as evidenced by nearly quantitative functionalization. Moreover, general agreement between the molecular weight of the clicked polymer **7** (M_n = 53315) and that of the precursor azide-polymer **6** (M_n = 42618) obtained by GPC also confirms efficient coupling. The observed increase in the molecular weight is due to the additional benzoxazine moiety incorporated.

It is also important to confirm whether benzoxazine ring will be preserved during the click reaction. The presence of signals in ^{1}H NMR spectra at 5.27 ppm and 4.55 ppm, corresponding to N—CH_2—O and N—CH_2-Ar clearly, indicates the retention of the benzoxazine ring during the click reaction [Fig. 1(B)]. Moreover, the characteristic absorption of benzoxazine structure appeares on copolymer **7** at 1,510, 1,226, 941 cm^{-1} also proves the existence of benzoxazine ring [Fig. 2(B)].

Preparation of the Single-Chain Nanoparticles via Intramolecular Crosslinking

As the crosslinking group should be selectively activated and react rapidly, an optimum reaction temperature to ensure

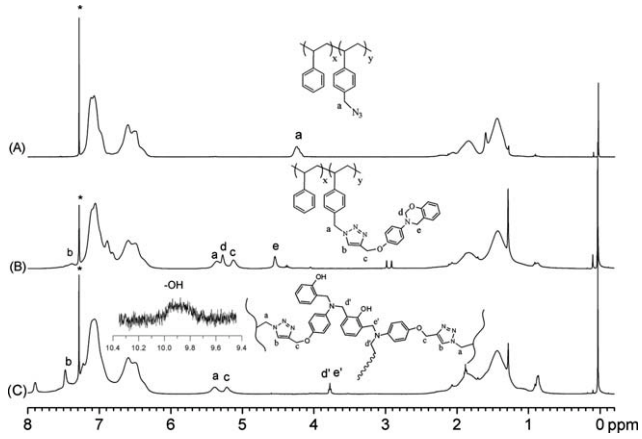

FIGURE 1 ^{1}H NMR spectra of (A) PS—N_3, (B) P(St-*co*-BS), and (C) nanoparticle **8**.

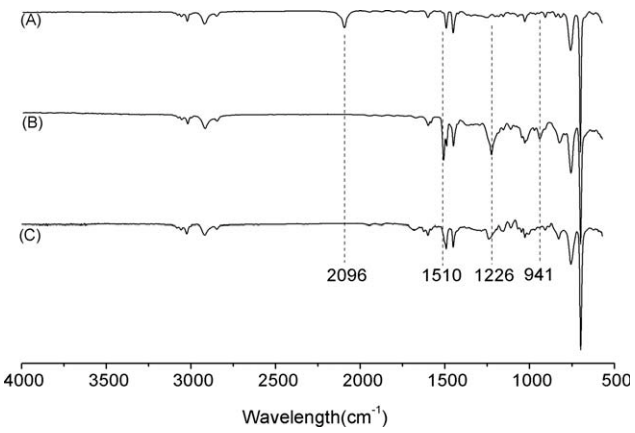

FIGURE 2 FTIR spectra of (A) PS—N_3, (B) P(St-*co*-BS), and (C) nanoparticle **8**.

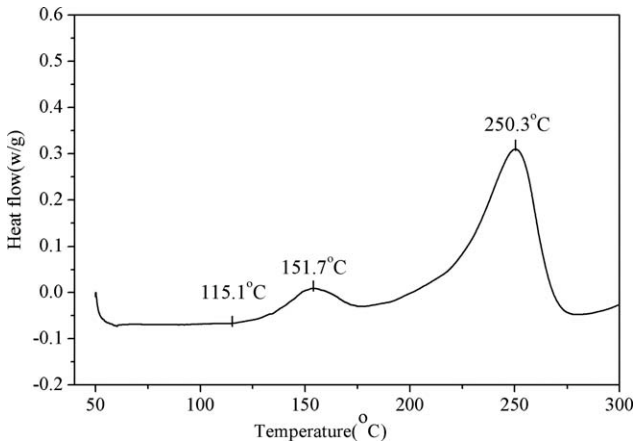

FIGURE 3 DSC thermogram of P(St-*co*-BS), **7**.

efficient and fast intramolecular crosslinking is very important. The DSC thermogram for copolymer **7** shown in Figure 3 reveals two exothermic peaks around 150 and 250 °C. In general, depending on the substituents and functional groups present in the structure, the benzoxazine ring opens at the temperature ranging between 210 and 250 °C. Thus, the exothermic peak at 250 °C corresponds to the ring-opening polymerization of benzoxazine moiety and results in the consequent crosslinking of the polymer. In addition to this exothermic peak, the thermogram shows an interesting feature of lower temperature exothermic peak with maximum value at 150 °C. Ishida et al.[21] attributed this phenomenon to the contribution from the thermal coupling of the residual propargyl and azide end groups. But Yagci et al.[22] gave the opinion that it may be due to the transformation of 1,2,3-triazole ring, because benzylic triazoles have the possibility to thermally transform from 1,2,3 form to other triazoles. Actually, there is limited information in the literature about the thermal stability of 1,2,3-triazole rings, formed via click chemistry, at elevated temperature. But the decomposition of the triazole ring by the evolution of nitrogen under 300 °C is impossible as no weight loss due to the nitrogen evolution was observed in thermogravimetric analysis (TGA) of polymer **7** (Fig. 4).

Considering the above factors, the intramolecular collapse of the single chain in dibenzyl ether at 250 °C (Scheme 3) and the dropwise technique described for benzocyclobutene[13] and sulfonyl azide[14] can be chosen. Under these conditions, the continuous addition strategy of a concentrated solution of the same linear polymer with a benzoxazine concentration of 0.02 M gives a final crosslinking concentration of 0.008 M in dibenzyl ether after addition.

The structure change from the random coil of linear polymers to intramolecular collapsed nanoparticles is monitored by ^{1}H NMR and FTIR. The disappearance of signals in ^{1}H NMR spectra at 5.27 ppm and 4.55 ppm corresponding to N—CH_2—O and N—CH_2-Ar clearly indicates the high-efficiency ring-opening reaction of the benzoxazine group at 250 °C [Fig. 1(C)], and the appearance of methylene protons at 3.7 ppm in Figure 1(C) proves the formation of the Mannich bridge structure[23] (-aromatic-CH_2—NR—CH_2-aromatic-) as described in Scheme 3. Moreover, the disappeared characteristic absorption of benzoxazine structure on nanoparticle **8** at 1,510, 1,226, 941 cm^{-1}, compared with that of polymer **7** also indicates the complete reaction of benzoxazine ring [Fig. 2(C)].

Comparison of the GPC traces for the collapsed nanoparticles versus the starting linear polymers is an efficient diagnostic technique for demonstrating the volume change that will be expected for the collapse of a linear polymer to give an intramolecularly crosslinked nanoparticle. As shown in Table 1, GPC data of the crosslinked nanoparticles show that the hydrodynamic volumes of the particles as measured by the elution time are significantly smaller than those of the starting linear polymers. The reduction in hydrodynamic volume and low polydispersity index indicate that no significant intermolecular crosslinking happens. For example, as shown in Figure 5, a copolymer with 10 mol % benzoxazine and an initial molecular weight M_n = 53315 (PDI = 1.38) gives a nanoparticle with a molecular weight M_n = 32522 (PDI = 1.30), which represents a reduction in hydrodynamic volume of 39%. This result agrees with the expected decrease in the size of the polymer due to the formation of the internal covalent bonds. As shown in Table 1, for styrenic copolymers containing 5, 10, 15, and 20 mol % benzoxazine-functionalized repeat units, a slightly increase in molecular weight is observed when the relative percentage of benzoxazine groups increases. After crosslinking, a systematic decrease in the hydrodynamic volume of the nanoparticles is observed on increasing the percentage of benzoxazine groups, which is consistent with an increase in the level of intramolecular bonding and a globular, three-dimensional (3D) structure. For the copolymers with the same amount of benzoxazine functionality, it can be found that the reduction in hydrodynamic volume after crosslinking becomes more obvious as the molecular weight of the linear polymers increases.

The Morphology and the Size of the Nanoparticles

Hydrodynamic radius (R_h) of the nanoparticles in tetrahydrofuran (THF) was determined by DLS. Examination of the data in Table 1 reveals that the size is very small

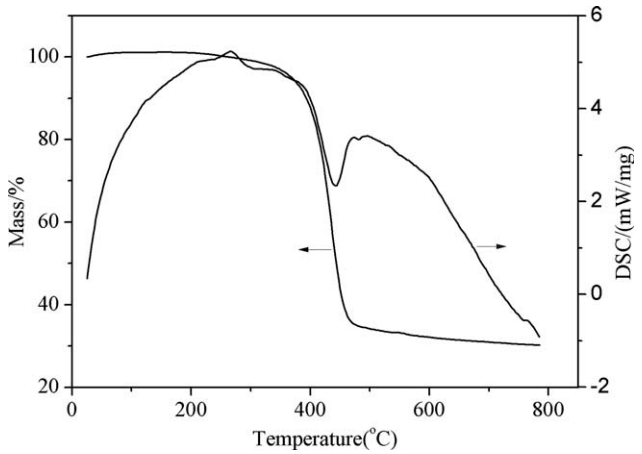

FIGURE 4 TGA-DTA thermogram of P(St-*co*-BS), **7**.

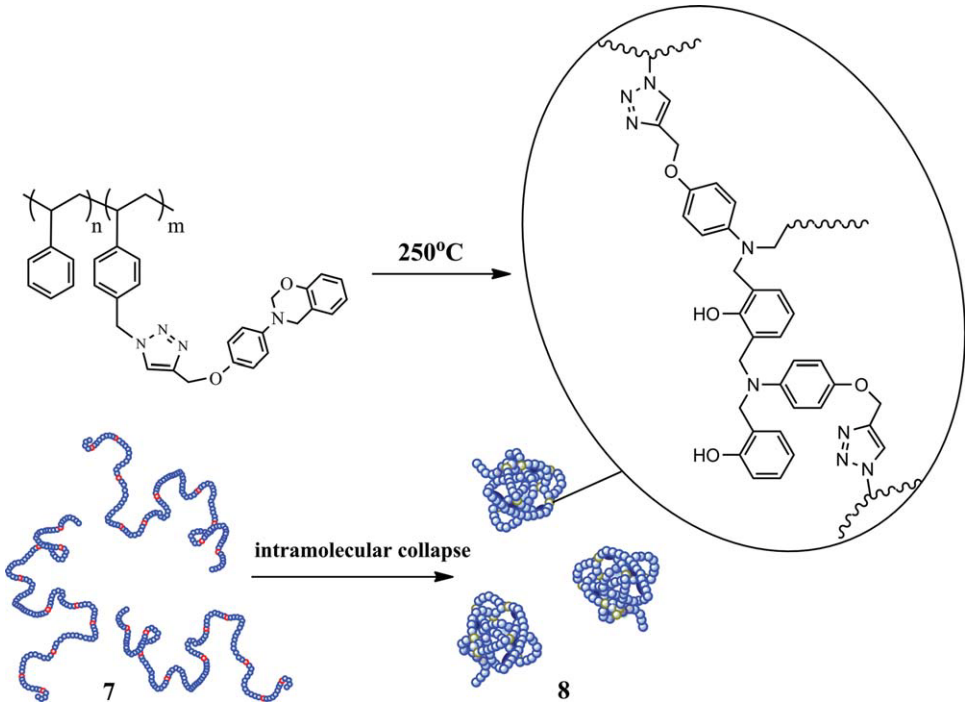

SCHEME 3 Schematic representation of the intramolecular collapse of linear polymer **7**, to give nanoparticle **8**.

(R_h = 5.1–11.8 nm). This range of size, which is characteristic of dendrimers and some micelles, has never been reached before for a polymeric nanoparticle via emulsion polymerization or self-assembly. Furthermore, the results also demonstrate the inherent versatility of this approach in controlling the size of the final nanoparticle. Not only can the size and the crosslinking density of the nanoparticle be controlled by the level of benzoxazine incorporated, but also the molecular weight of the starting linear polymer plays a key role in determining the hydrodynamic size of the final nanoparticle. All these factors can be regulated by the use of controlled polymerization techniques.

The 3D morphology of the polymeric nanoparticles on the solid substrate was measured by atomic force microscopy (AFM). The samples were dissolved in THF, and all solutions were filtered with a Teflon filter (0.2 μm) to reduce the amount of large dust particles and atmospheric

TABLE 1 Comparison of GPC and DLS Data for PS—N_3, **6**, P(St-*co*-BS), **7**, and the Final Nanoparticle, **8**

Precursors (PS—N_3)			Linear Polymers [P(St-*co*-BS)]		Nanoparticles		
—N_3[a] mol % (%)	M_n	PDI	M_n	PDI	M_n	PDI	R_h[b] (nm)
5	22,474	1.22	25,782	1.31	21,156	1.25	6.6
10	23,093	1.27	28,618	1.37	19,475	1.27	6.1
15	23,441	1.29	32,210	1.33	17,265	1.31	5.7
20	25,100	1.33	38,465	1.46	16,924	1.39	5.1
5	41,533	1.21	46,932	1.33	36,484	1.22	8.7
10	42,618	1.23	53,315	1.38	32,522	1.30	7.8
15	44,382	1.19	60,433	1.31	24,365	1.21	7.1
20	44,654	1.37	64,620	1.48	22,838	1.38	6.8
5	71,580	1.24	80,269	1.45	52,174	1.31	11.8
10	73,497	1.41	91,283	1.62	46,513	1.44	10.6

[a] Mole fraction of N_3 units as measured by ^{1}H NMR.
[b] Hydrodynamic radius as measured by DLS in THF at the concentration of 0.1 mg/mL.

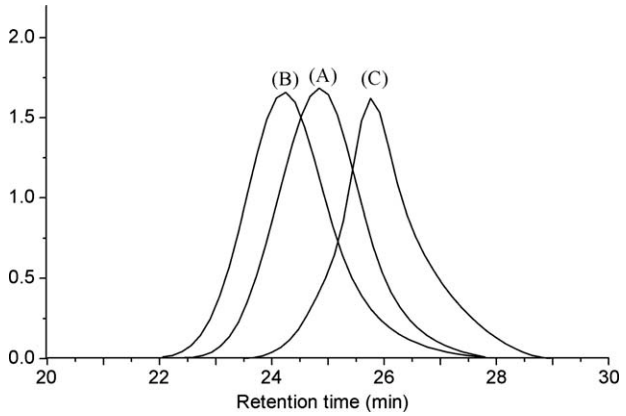

FIGURE 5 GPC traces for (A) PS—N_3, **6**, (M_n = 42618, PDI = 1.23), (B) P(St-*co*-BS), **7**, (M_n = 53315, PDI = 1.38), and (C) nanoparticle **8** (M_n = 32522, PDI = 1.30).

contaminants. The solution (concentration, 0.01 mg/mL) was spin-coated at 2000 rpm for 40 s on the mica substrate. The images shown in Figure 6 clearly demonstrate the uniformity of the nanoparticles on the surfaces, and the narrow height distribution provides evidence that only individual polystyrene nanoparticles are present and no agglomeration of nanoparticles occurs. It is clear that the dimension of the nanoparticles increases with increasing molecular weight of the starting linear polymer.

As shown in Figure 7(A), the diameter of the nanoparticle (12.5 ± 1.5 nm) is much larger than its height (1.6 ± 0.3 nm) on the mica surface. Thus, on the mica surface the nanoparticle adopts a pancake-like shape as shown in the inset of Figure 7(A). This pancake-like conformation is also observed in dendrimer structure. It has been shown before that both charged and uncharged dendrimers are adsorbed to mica surface and form a flat disk structure.[24] With a high free energy surface like mica, the number of the repeat units in contact with the surface will increase to gain adsorption energy to reduce the conformational entropy, therefore, the height of the nanoparticle on the substrate will be smaller than its unperturbed size.[25] Further evaluation of the collapsed nanoparticles with transmission electron microscope (TEM) confirms the controlled crosslinking process of linear precursors into defined 3D architectures with the mean diameter of 8.7 ± 1.5 nm (Fig. 8).

EXPERIMENTAL

Materials

N-(4-hydroxyphenyl)acetamide, tetrabutylammonium bromide, paraformaldehyde, HCl solution (37%), CuBr, ethanol, methanol, PMDETA, phenol, 1,4-dioxane, chloroform, toluene, THF, DMF, diethyl ether, sodium hydroxide, anhydrous magnesium sulfate, and sodium azide were all analytical grades and purchased from Shanghai Chemical Reagent. Propargyl bromide (~80 volume % in toluene), CMS (90%) and benzyl ether (98%) were obtained from Aldrich. St and CMS were distilled under reduced pressure before use. AIBN was recrystallized from ethanol. THF was dried with sodium using benzophenone as indicator. CuBr was purified by washing with acetic acid and acetone alternately. The RAFT agent ECPDB was prepared similar to the method described in reference.[26] All other reagents were used without further purification.

Synthesis of APPE, 3

The synthesis of APPE is similar to the method described in Ref. [22]. In a 250-mL flask, N-(4-hydroxyphenyl)acetamide, **1**, (8.1 g, 50 mmol) was dissolved in 100-mL NaOH solution (0.4 N) and heated at 70 °C until a clear solution was formed. Then tetrabutylammonium bromide (1.6 g, 5 mmol) was added as a phase transfer catalyst. A solution of propargyl bromide (6.5 g, 55 mmol) in 50-mL toluene was added portion-wise to the solution and stirred at 70 °C for 24 h. Then, it was cooled to get the solid product, and the toluene layer was separated, washed repeatedly with water, and precipitated. The crude product was dissolved in 1,4-dioxane and precipitated in water (ca. 200 mL), and washed repeatedly with copious amount of water to give N-(4-(prop-2-ynyloxy)phenyl)acetamide, **2**,

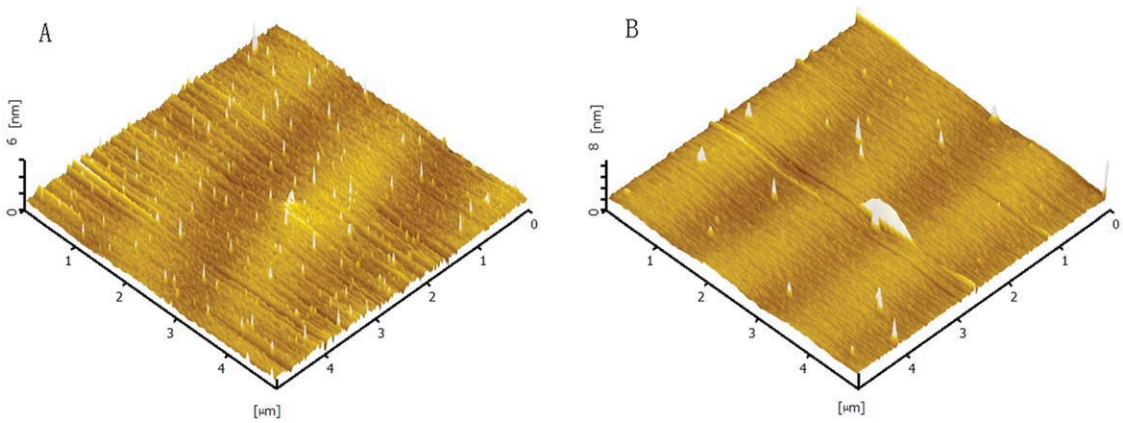

FIGURE 6 AFM 3D images of nanoparticle 8, the image dimensions are both 5 × 5 μm. (A) 10 mol % benzoxazine, M_n = 19475, PDI = 1.27; (B) 10 mol % benzoxazine, M_n = 46513, PDI = 1.44.

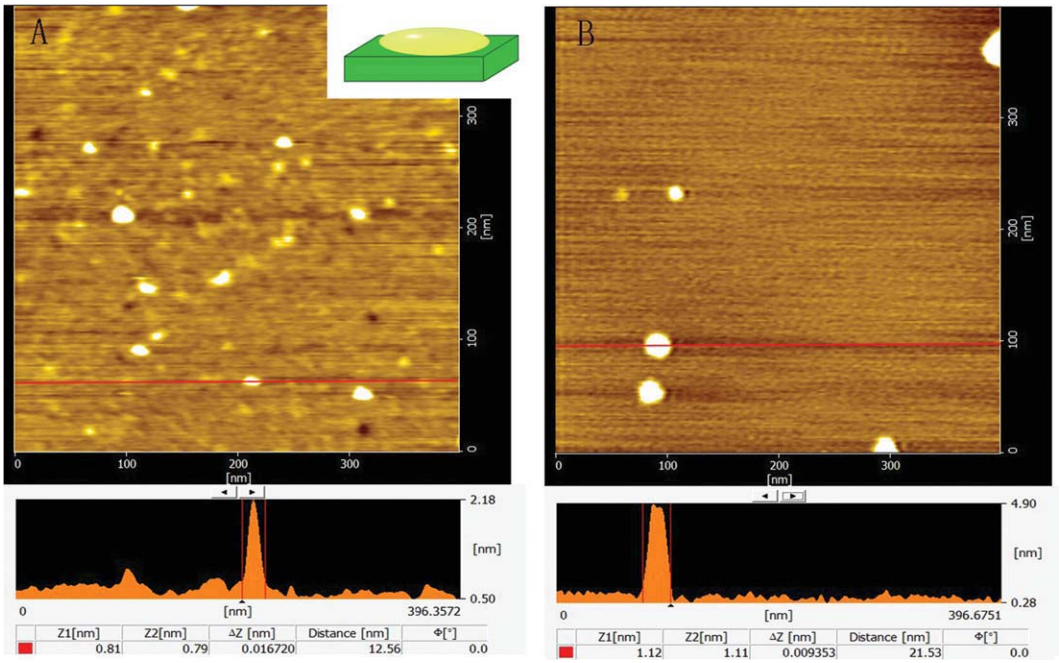

FIGURE 7 Top-view of AFM images of nanoparticle **8** and the sectional analysis of the single nanoparticle; (A) 10 mol % benzoxazine, M_n = 19475, PDI = 1.27; (B) 10 mol % benzoxazine, M_n = 46513, PDI = 1.44; The inset shows a pancake-like model.

(8.9 g, yield: 94 %). In a 250 mL flask, **2** (8.5 g, 45 mmol) was dissolved in 70-mL ethanol, and then 70-mL HCl solution (37%) was added. The mixture was stirred at 90 °C for 3 h.

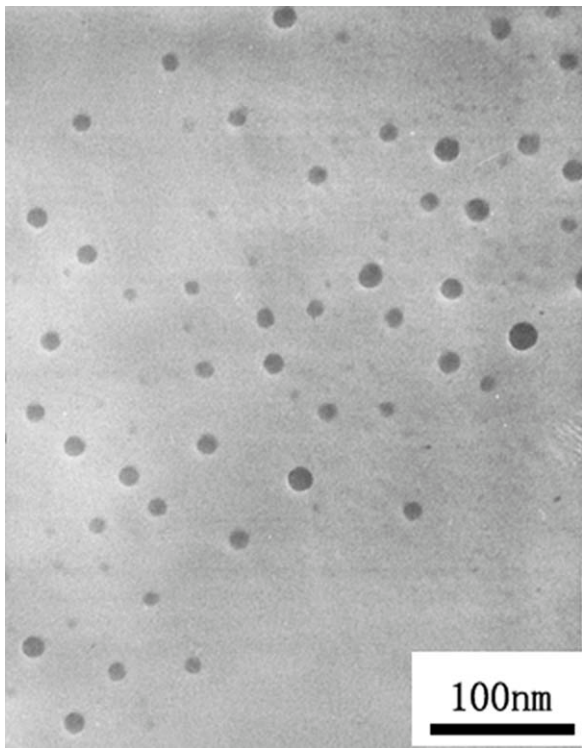

FIGURE 8 TEM image of nanoparticle **8** (10 mol % benzoxazine, M_n = 46513, PDI = 1.44).

After neutralized with sodium hydroxide, the solution was extracted with chloroform, and the organic layer was dried over anhydrous $MgSO_4$. Evaporation of chloroform gave a yellowish brown viscous product. The crude product was purified by distillation under reduced pressure (bp: 95 °C, 10 mmHg) to get a colorless and highly viscous liquid, which crystallized into yellowish white crystals after a while in the flask to APPE, **3**, (5.0 g, yield: 75 %, mp: 49–50 °C). ^{1}H-NMR (400 MHz, $CDCl_3$, δ):2.50 (t, ≡C—H), 3.50 (br s, NH_2), 4.60 (d, CH_2, propargyl), 6.65–6.81 (d, d, 4H, Ar).

Synthesis of P-APPE, 4

Into a 20-mL vial APPE (1.47 g, 10 mmol), phenol (0.94 g, 10 mmol), and paraformaldehyde (0.90 g, 30 mmol) were mixed together and heated at 120 °C for 20 min. The crude product after cooling was dissolved in 50-mL diethyl ether and washed several times with 1 N sodium hydroxide solution and finally with distilled water. Then, the ether solution was dried with anhydrous sodium sulfate, followed by evaporation of ether under vacuum to get pale yellow viscous fluid. (1.59 g, yield: 60%). FTIR (ν, cm^{-1}): 3,290, 3,041, 2,919, 2,121, 1,597, 1,506, 1,336, 1,236, 1,217, 1,034, 1,019, 954, 756, 690, 642. ^{1}H NMR (400 MHz, $CDCl_3$, δ): 2.50 (t, ≡C—H), 4.55 (s, CH_2, oxazine), 4.61 (d, CH_2, propargyl), 5.29 (s, CH_2, oxazine), and 6.75–7.1 (8H, Ar).

Synthesis of P(St-*co*-CMS), 5

P(St-*co*-CMS) containing quantitative chloromethyl groups was synthesized via RAFT polymerization of St and CMS in the presence of ECPDB and AIBN. To a Schlenk tube equipped with a magnetic stirring bar, styrene (1.8747 g, 18.0 mmol), CMS (0.3052 g, 2.0 mmol), ECPDB (0.0063 g,

0.02 mmol), and AIBN (0.0016 g, 0.01 mmol) were added in that order. The tube was degassed by three freeze-pump-thaw cycles, left in vacuum, and placed in oil bath at 65 °C for 12 h. Subsequently, the mixture of the polymerization was diluted with THF and precipitated in excess methanol. The polymer was dried for 24 h in a vacuum oven at 25 °C to give **5**, as a pink powder (1.00 g, yield: 45%). FTIR (ν, cm^{-1}): 3,050, 2,924, 1,601, 1,492, 1,452, 1,265, 757, and 699. ^1H NMR (400 MHz, $CDCl_3$, δ): 7.24–6.25 (m, Ar), 4.50 (br s, CH_2), 1.23–2.13 (m, CH_2, CH).

Synthesis of PS—N_3, 6

Copolymer **5** was dissolved in DMF, and then NaN_3 (two times excess to the mole of chloromethyl group of each copolymer) was added. The resulting solution was allowed to stir at 25 °C overnight and precipitated into methanol/water mixture (1/1 by volume). After filtration, the polymer was dried for 24 h in a vacuum oven at 25 °C to give **6**, as a colorless powder (yield: 92%). FTIR (ν, cm^{-1}): 3,026, 2,924, 2,096, 1,681, 1,601, 1,493, 1,452, 907, 757, and 699. ^1H NMR (400 MHz, $CDCl_3$): δ = 7.24–6.23 (m, Ar), 4.25 (br s, CH_2), 2.21–1.22 (m, CH_2, CH).

Synthesis of P(St-*co*-BS), 7

Copolymer **6** (0.5 g, 0.46 mmol —N_3, M_n = 42618, PDI = 1.23), and P-APPE (0.24 g, 0.92 mmol) were dissolved in 10-mL DMF in a Schlenk tube and purged with nitrogen. CuBr (0.26 g, 1.84 mmol) and PMDETA (0.31 g, 2 mmol) were added, and the reaction mixture was degassed by three freeze-pump-thaw cycles and left under nitrogen and stirred at room temperature for 24 h. Subsequently, the polymer solution was precipitated into methanol and then dissolved in THF and passed through an alumina column to remove copper salt. Finally, the polymer solution was concentrated and precipitated in excess methanol, then filtered and dried under vacuum to give **7**, as beige powder (0.57 g, yield: 92%). FTIR (ν, cm^{-1}): 3,026, 2,924, 1,601, 1,510, 1,493, 1,452, 1,226, 1,030, 941, 755, and 699. ^1H NMR (400 MHz, $CDCl_3$, δ): 7.38 (br s, CH=C), 7.24–6.23 (m, Ar), 5.36 (br s, CH_2), 5.27 (br s, CH_2), 5.12 (br s, CH_2), 4.55 (br s, CH_2), 2.21–1.22 (m, CH_2, CH).

General Procedure for the Preparation of the Nanoparticle

In a 100-mL three-necked flask equipped with an internal thermometer, 25 mL of benzyl ether was heated at 250 °C under nitrogen. A solution of 0.5 g benzoxazine-functionalized linear copolymer **7** (M_n = 53315, PDI = 1.38, 10 mol % benzoxazine) dissolved in 20 mL benzyl ether, was added dropwise via a peristaltic pump at about 12 mL/h with vigorously stirring. After addition, the reaction mixture was heated for an additional 2.5 h, the polymer mixture was concentrated and precipitated in excess methanol. After filtration, the polymer was dried for 24 h in a vacuum oven at 25 °C to give the nanoparticle **8**, as a beige powder (0.45 g, yield: 90%). FTIR (ν, cm^{-1}): 3,025, 2,918, 1,679, 1,601, 1,493, 1,452, 1,241, 1,028, 829, 755 and 699. ^1H NMR (400 MHz, $CDCl_3$, δ): 9.90 (br s, OH), 7.38 (br s, CH=C), 7.24–6.23 (m, Ar), 5.39 (br s, CH_2), 5.22 (br s, CH_2), 3.77 (br s, CH_2), 2.21–1.22 (m, CH_2, CH).

Characterization

^1H NMR measurements were carried out on a Bruker AMX 300 spectrometer, $CDCl_3$ as the solvent. FTIR analysis of the samples was carried out on a thermo Bruker EQUINOXSS/HYPERION 2000 spectrometer. GPC was performed in THF on a Waters Alliance HPLC system. The molecular weight of the polymers was calculated relative to linear polystyrene standard. DSC of the polymers was performed on MDSC-Q100 (TA) under a nitrogen atmosphere at a constant heating rate of 10 °C/min. TGA was performed on a STA 449C (NETZSCH Co.) instrument under a nitrogen atmosphere at a constant heating rate of 20 °C/min. TEM was performed with a Hitachi H-600 TEM, operating with an acceleration voltage of 200 KV. The TEM samples were prepared by placing one drop of the diluted dispersion of the nanoparticles on a 200 mesh carbon coated copper grid and left in air to dry. The height and distribution of the nanoparticles were determined on tapping-mode AFM (SPA-300HV, Seiko Instruments) under ambient condition in air. The standard silicon tips were used. The average particle size of the nanoparticles was also determined on Malvern Autosizer 4700 dynamic light scattering (DLS) equipped with a solid-state laser (ILT 5500QSL, output power 100 mW at λ = 532 nm) as light source.

CONCLUSIONS

In summary, a new synthetic strategy for the controlled intramolecular crosslinking of linear polymers with pendant benzoxazine groups to give single-chain nanoparticles has been demonstrated. It is found that the dimension of the polymeric nanoparticles can be controlled in 5–20 nm by varying the molecular weight and the amount of benzoxazine groups for the starting linear polymers. It is also confirmed that the nanoparticles adopt a pancake-like shape on a high free energy surface. Furthermore, a wide range of benzoxazine monomers with additional functionalities such as acetylene, nitrile, propargyl, and maleimide groups can be easily prepared from inexpensive raw materials, this flexibility provides much possibility of incorporating benzoxazine group into polymer to give the crosslinkable precursors to prepare single-chain nanoparticles.

The project is sponsored by Major Program for Fundamental Research of Shanghai Science & Technology Commission (09JC1414300) and Natural Science Foundation of China (21144006)

REFERENCES AND NOTES

1 (a) Gillies, E. R.; Frechet, J. M. J. Drug Discovery Today 2005, 10, 35–43; (b) Kumari, A.; Yadav, S. K.; Yadav, S. C. Colloids Surfaces B-Biointerfaces 2010, 75, 1–20; (c) Tuteja, A.; Mackay, M. E.; Hawker, C. J.; Van Horn, B. Macromolecules 2005, 38, 8000–8011.

2 Johan Foster, E.; Berda E. B.; Meijer, E. W. J Polym Sci Part A: Polym Chem 2011, 49, 118–126.

3 (a) Hawker, C. J.; Hedrick, J. L.; Miller, R. D.; Volksen, W. MRS Bull 2000, 25, 54–58; (b) Yang, S.; Mirau, P. A.; Pai, C. S.; Nalamasu, O.; Reichmanis, E.; Lin, E. K.; Lee, H. J.; Gidley, D. W.; Sun, J. N. Chem Mater 2001, 13, 2762–2764.

4 Li, M.; Zhang, Y. B.; Jiang, M.; Zhu, L.; Wu, C. Macromolecules 1998, 31, 6841–6844.

5 Moraes, C. M.; de Lima, R.; Rosa, A. H.; de Paula, E.; Fraceto, L. F. Macromol Symposia 2009, 281, 106–112.

6 (a) Huang, H. Y.; Remsen, E. E.; Kowalewski, T.; Wooley, K. L. J Am Chem Soc 1999, 121, 3805–3806; (b) Lee, N. S.; Lin, L. Y.; Neumann, W. L.; Freskos, J. N.; Karwa, A.; Shieh, J. J.; Dorshow, R. B.; Wooley, K. L. Small 2011, 7, 1998–2003.

7 Foster, E. J.; Berda, E. B.; Meijer, E. W. J Am Chem Soc 2009, 131, 6964–6966.

8 (a) Pavel, F. M. J Disper Sci Tech 2004, 25, 1–16; (b) Xu, X. J.; Gan, L. M. Curr Opin Colloid Interface Sci 2005, 10, 239–244.

9 (a) Crooks, R. M.; Zhao, M. Q.; Sun, L.; Chechik, V.; Yeung, L. K. Accounts Chem Res 2001, 34, 181–190; (b) Scott, R. W. J.; Wilson, O. M.; Crooks, R. M. J Phys Chem B 2005, 109, 692–704.

10 (a) Martin, J. E.; Eichinger, B. E. Macromolecules 1983, 16, 1345–1350; (b) Martin, J. E.; Eichinger, B. E. Macromolecules 1983, 16, 1350–1358; (c) Antonietti, M.; Pakula, T.; Bremser, W. Macromolecules 1995, 28, 4227–4233; (d) Davankov, V. A.; Ilyin, M. M.; Tsyurupa, M. P.; Timofeeva, G. I.; Dubrovina, L. V. Macromolecules 1996, 29, 8398–8403.

11 (a) Jiang, J.; Thayumanavan, S. Macromolecules 2005, 38, 5886–5891; (b) Mecerreyes, D.; Lee, V.; Hawker, C. J.; Hedrick, J. L.; Wursch, A.; Volksen, W.; Magbitang, T.; Huang, E.; Miller, R. D. Adv Mater 2001, 13, 204–208.

12 de Luzuriaga, A. R.; Ormategui, N.; Grande, H. J.; Odriozola, I.; Pornposo, J. A.; Loinaz, I. Macromol Rapid Commun 2008, 29, 1156–1160.

13 Harth, E.; Van Horn, B.; Lee, V. Y.; Germack, D. S.; Gonzales, C. P.; Miller, R. D.; Hawker, C. J. J Am Chem Soc 2002, 124, 8653–8660.

14 Jiang, X. Y.; Pu, H. T.; Wang, P. Polymer 2011, 52, 3597–3602.

15 Croce, T. A.; Hamilton, S. K.; Chen, M. L.; Muchalski, H.; Harth, E. Macromolecules 2007, 40, 6028–6031.

16 Beck, J. B.; Killops, K. L.; Kang, T.; Sivanandan, K.; Bayles, A.; Mackay, M. E.; Wooley, K. L.; Hawker, C. J. Macromolecules 2009, 42, 5629–5635.

17 Njikang, G.; Liu, G. J.; Curda, S. A. Macromolecules 2008, 41, 5697–5702.

18 (a) Yagci, Y.; Kiskan, B.; Ghosh, N. N. J Polym Sci Part A: Polym Chem 2009, 47, 5565–5576; (b) Velez-Herrera, P.; Ishida, H. J Polym Sci Part A: Polym Chem 2009, 47, 5871–5881; (c) Kiskan, B.; Aydogan, B.; Yagci, Y. J Polym Sci Part A: Polym Chem 2009, 47, 804–811.

19 Ghosh, N. N.; Kiskan, B.; Yagci, Y. Prog Polym Sci 2007, 32, 1344–1391.

20 (a) Kolb, H. C.; Finn, M. G.; Sharpless, K. B. Angew Chem Int Ed Engl 2001, 40, 2004–2021; (b) Binder, W. H.; Sachsenhofer, R. Macromol Rapid Commun 2007, 28, 15–54; (c) Moses, J. E.; Moorhouse, A. D. Chem Soc Rev 2007, 36, 1249–1262; (d) Thibault, R. J.; Takizawa, K.; Lowenheilm, P.; Helms, B.; Mynar, J. L.; Frechet, J. M. J.; Hawker, C. J. J Am Chem Soc 2006, 128, 12084–12085.

21 Chernykh, A.; Agag, T.; Ishida, H. Polymer 2009, 50, 382–390.

22 Ergin, M.; Kiskan, B.; Gacal, B.; Yagci, Y. Macromolecules 2007, 40, 4724–4727.

23 (a) Ishida, H.; Rodriguez, Y. Polymer 1995, 36, 3151–3158; (b) Ishida, H.; Krus, C. M. Macromolecules 1998, 31, 2409–2418.

24 (a) Taranekar, P.; Park, J. Y.; Patton, D.; Fulghum, T.; Ramon, G. J.; Advincula, R. Adv Mater 2006, 18, 2461–2465; (b) Mecke, A.; Lee, I.; Baker, J. R.; Holl, M. M. B.; Orr, B. G. Eur Phys J E 2004, 14, 7–16.

25 Dukette, T. E.; Mackay, M. E.; Horn, B. V.; Wooley, K. L.; Drockenmuller, E.; Malkoch, M.; Hawker, C. J. Nano Lett 2005, 5, 1704–1709.

26 Perrier, S.; Takolpuckdee, P.; Westwood, J.; Lewis, D. M. Macromolecules 2004, 37, 2709–2717.